

RESEARCH ARTICLE

Effect of support hydrophobicity of halloysite-based catalysts on the polyalphaolefin hydrofinishing performance

Arash Shams¹  | Samahe Sadjadi²  | Josep Duran³  | Sílvia Simon³  |
Albert Poater³  | Naeimeh Bahri-Laleh⁴ 

¹Department of Polymer Engineering and Color Technology, Amirkabir University of Technology, Tehran, Iran

²Gas Conversion Department, Faculty of Petrochemicals, Iran Polymer and Petrochemical Institute, Tehran, Iran

³Institut de Química Computational i Catalísi and Department of Chemistry, University of Girona, Girona, Spain

⁴Polymerization Engineering Department, Iran Polymer and Petrochemical Institute (IPPI), Tehran, Iran

Correspondence

Albert Poater, Institut de Química Computational i Catalísi and Department of Chemistry, University of Girona, c/Maria Aurèlia Capmany 69, 17003 Girona, Catalonia, Spain.

Email: albert.poater@udg.edu

Samahe Sadjadi, Gas Conversion Department, Faculty of Petrochemicals, Iran Polymer and Petrochemical Institute, P.O. Box 14975-112, Tehran, Iran.

Email: s.sadjadi@ippi.ac.ir

Naeimeh Bahri-Laleh, Polymerization Engineering Department, Iran Polymer and Petrochemical Institute (IPPI), P.O. Box 14965/115, Tehran, Iran.

Email: n.bahri@ippi.ac.ir

Funding information

Institució Catalana de Recerca i Estudis Avançats, Grant/Award Number: ICREA Academia 2019; Spanish MINECO, Grant/Award Number: PGC2018-097722-B-I00; Iran Polymer and Petrochemical Institute

Abstract

Hydrogenation of polyalphaolefins (PAOs) is an industrial process catalyzed by supported precious metals. In this regard, halloysite (Hal) clay has been proven as an efficient support for the immobilization of Pd nanoparticles and development of high-performance catalysts under mild reaction condition. In this research, the effect of Hal hydrophobicity on the PAO hydrofinishing efficiency is studied. In this line, cetrimonium bromide (CTAB) was used for adjusting the hydrophobicity of halloysite surface. Three catalysts, Hal/Pd, Hal/Pd/CTAB, and Hal/CTAB/Pd, were fabricated by palladation of Hal, treating palladated Hal with CTAB and palladation of CTAB-treated Hal, respectively. The catalysts were characterized, and their activity for the hydrogenation of PAO was appraised. Moreover, a molecular simulation approach was employed to survey the effect of surface hydrophobicity of Hal on the alkene hydrogenation energy diagram and the steric maps of the main catalytic stages. Both experimental and computational studies approved that the presence of CTAB detracts the activity of the catalyst. Moreover, the order of introduction of Pd and CTAB affects the content of incorporated CTAB and Pd and Pd particle size, and the order of catalysts activity was as follows: Hal/Pd > Hal/Pd/CTAB > Hal/CTAB/Pd. In fact, 5 wt.% Hal/Pd promoted the hydrogenation at 130°C and hydrogen pressure of 8 bar to furnish 98% hydrogenated PAO.

KEYWORDS

catalyst, DFT, halloysite, hydrofinishing, polyalphaolefin

This is an open access article under the terms of the [Creative Commons Attribution](https://creativecommons.org/licenses/by/4.0/) License, which permits use, distribution and reproduction in any medium, provided the original work is properly cited.

© 2022 The Authors. *Applied Organometallic Chemistry* published by John Wiley & Sons Ltd.

1 | INTRODUCTION

As heterogeneous catalysis is an appealing topic from an industrial point of view,^[1–3] it has witnessed immense advances in recent decades, and a myriad type of heterogeneous catalysts has been devised using several supporting materials. More recently, single atom catalysts systems have appeared as a way to go from the precision of homogeneous catalysis to the effectivity of heterogeneous catalysis.^[2,4,5] In this context, natural and readily available supports, such as clays, have received massive attention, and the usefulness of various clays for designing catalytic systems has been disclosed.

One of the least known members of Kaolin clay group is halloysite (Hal). This dioctahedral 1:1 clay^[6–10] has recently been the focus of research for a wide range of applications,^[11–13] such as catalysis, cleaning,^[14] adsorbent,^[15] delivery systems, packaging,^[16] etc. The extensive utility of Hal as well as its excellent performance can be attributed to its unique physicochemical properties, such as tubular morphology with a relatively high lumen space (11%–39%),^[17,18] oppositely charged inner and outer surface, aspect ratio of 10–50 and average pore size of 79.7–100.2 Å.^[19–21] Furthermore, both surfaces of Hal can be modified through covalent or non-covalent approaches.^[22–24] This leads a broad scope of uses for halloysites, from the bio field,^[25,26] resulted in rapid growth of Hal-based catalysts for various chemical reactions,^[27] including hydrogenation^[28,29] and oxidation reactions,^[30] as well as synthesis of organic compounds.^[31,32]

Polyalphaolefin (PAO)-type lubricants synthesized from long α -olefin monomers, generally from C6 to C12, is of the group IV of the American Petroleum Institute (API) category.^[33–35] Their unique properties, such as high oxidation stability and viscosity index (VI),^[36,37] and extremely low pour point render them distinguished ones among all synthetic oils categories.^[38] Statistically, more than 42% of the sum of synthetic oil market belongs to PAO grades.^[39] Despite facile synthesis routes and immense developments in industrial production sector, the crude PAO still suffers from the existence of —C=C— double bonds in its backbone.^[40,41] These bonds make PAO susceptible to cleavage at high temperature of application, which deteriorates PAOs unique characteristics and decreases its shelf life.^[42,43] To overcome this drawback, PAO hydrofinishing, as an essential stage in its production, is usually accomplished. This stage needs harsh environment with high temperature and H_2 pressure (nearly above 200°C and 25 bar), which increases the risk and cost of PAO production. Therefore, finding appropriate catalysts for PAO hydrofinishing that can perform

this reaction at mild reaction condition is always the topic of research in academia and industry.

In the continuation of our research on Hal-based catalysts for hydrogenation reactions,^[44–47] herein, and knowing that the presence of protic solvents and reagents is detrimental for this reaction,^[48–50] we wish to report a combined computational and experimental study on the effect of the hydrophobicity of Hal on its performance for hydrofinishing of PAO.

2 | EXPERIMENTAL

2.1 | Chemicals and solvents

Preparation of the catalysts in this research was fulfilled using the following chemicals and solvents (all provided from Sigma-Aldrich), Hal, cetrimonium bromide (CTAB), Pd (OAc)₂, NaBH₄, AgNO₃ (Silver nitrate), toluene, and methanol (MeOH). The materials used for the synthesis of PAO (all purchased from Merck Co. Germany) included 1-decene, AlCl₃, and NaOH.

2.2 | Instruments

The analyses and the applied instruments for the characterization of the as-prepared catalysts are as follow: Inductively coupled plasma (ICP) was performed by using Varian, Vista-pro for calculating the content of Pd in all three samples. Transmission electronic microscopy (TEM) was carried out (Philips100 Kv AMBS) to investigate the morphology of the synthesized samples. Fourier transform infrared (FTIR) spectra of the as-prepared samples were recorded on PERKIN-ELMER Spectrum 65 using the KBr pellet. Thermogravimetric analysis (TGA) of the catalysts was conducted on METTLER TOLEDO apparatus under oxygen atmosphere, with a heating rate of 10°C/min. Contact angles of the catalysts were studied at ambient temperature using a Dino-Lite Plus camera. The captured images were examined with an image processing software (Digimizer). To record the X-ray diffraction (XRD) patterns, Siemens, D5000 armed with a Cu K α radiation was applied. The energy dispersive X-ray spectrum (EDS) and elemental analysis were performed using a MIRA 3 TESCAN-XMU. The Brunauer–Emmet–Teller (BET) surface area of Hal and the catalysts were estimated using the Belsorp Mini II apparatus. Zeta potential measurement was carried out in water suspension using a Horiba SZ-100 apparatus.

To determine the yield of hydrofinishing, the hydrogenated PAO was analyzed by nuclear magnetic

resonance (^1H NMR) spectroscopy. To perform the analysis, Bruker DRX 400 MHz instrument was used and the sample was dissolved in chloroform.

2.3 | Preparation of the catalyst

2.3.1 | Synthesis of Hal/Pd

To immobilize Pd nanoparticles on Hal, Hal (2 g) was dispersed in toluene (30 ml) under ultrasonic irradiation (power of 150 W for 5 min). Separately, a solution of Pd(OAc)₂ (3 wt.%) in toluene (5 ml) was prepared and slowly added to the as-prepared Hal suspension under Ar atmosphere. After 2 h, a NaBH₄ solution in MeOH (2 M) was gently introduced to the aforementioned stirring suspension. Stirring was continued for 5 h to ensure reduction of Pd(II) to Pd(0). Finally, the resulting precipitate was centrifuged, washed with MeOH, and then dried at 60°C overnight.

2.3.2 | Synthesis of Hal/Pd/CTAB

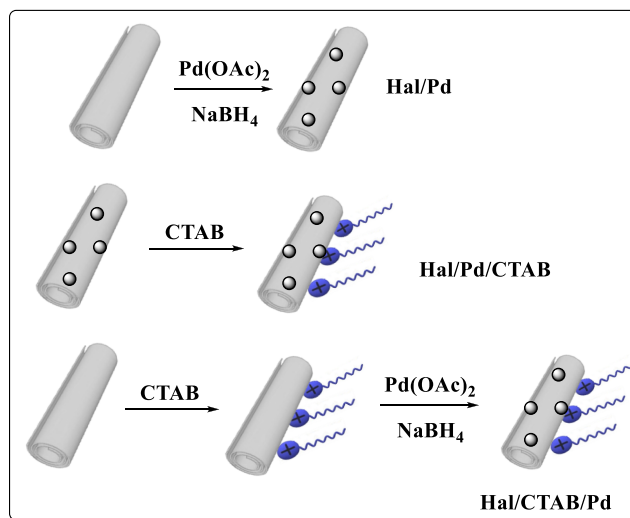
To prepare Hal/Pd/CTAB, Hal was first palladated using the similar procedure used for the synthesis of Hal/Pd sample (see Section 2.3.1).^[51,52] Then, the as-prepared Hal/Pd was modified with CTAB according to the previous report.^[53] Briefly, a solution of CTAB (0.5 g) in distilled water was prepared. Then, Hal/Pd (1 g) was added, and the resulting mixture was stirred for 2 days. Afterwards, the precipitate was separated via centrifugation and washed repeatedly with distilled water. To assure removal of free CTAB, aqueous solution of AgNO₃ was applied. Finally, the resulting solid was dried at 80°C for 1 week.

2.3.3 | Synthesis of Hal/CTAB/Pd

Hal/CTAB/Pd was prepared through a similar procedure applied for the synthesis of Hal/Pd/CTAB, except Hal was first modified with CTAB and then palladated. The procedures for the synthesis of the catalysts are presented in Scheme 1.

2.4 | Synthesis of PAO

Oligomerization of 1-decene and synthesis of PAO was carried out according to the literature.^[27] Typically, the reactor used for the polymerization was first charged with AlCl₃ (5 g) and purged with an inert gas. After



SCHEME 1 Employed procedures for the synthesis of the designed catalysts

heating at 80°C for 1 h, 1-decene (500 g) and deionized water (0.3 ml) were added, and the reaction mixture was stirred for 50 min at 100°C. At the end of the reaction, the obtained oil was rinsed several times with 5 wt.% NaOH. Further purification was achieved by heating of the mixture under a 0.8 bar vacuum to 250°C. The yield of PAO synthesis was estimated to be 86%.

2.5 | Hydrogenation of PAO

Hydrofinishing of PAO was conducted in a stainless steel reactor equipped with regulators, a circulator and a magnetic stirrer. Prior to the reaction, the reactor was purged with N₂ gas and heated at 100°C for 1 h. Afterwards, the as-synthesized PAO (10 g) and the catalyst (5 wt.%) were transferred to the reactor. Then, the reactor was sealed, H₂ gas pressure was set on 8 bar, and the reaction temperature was elevated to 130°C. The reaction mixture was continuously stirred under the aforesaid condition for 8 h. Upon completion of the reaction, the reactor was cooled, and the catalyst was simply separated via centrifugation. Then, the yield of hydrofinishing was estimated by ^1H NMR spectroscopy.

2.6 | Recovery and recycling of the catalyst

To recover the collected catalyst, it was first washed with n-hexane for three times to remove deposited oil on its surface. Then, the washed catalyst was dried at 60°C overnight and applied for the next run of the hydrofinishing reaction.

2.7 | Computational details

Density functional theory (DFT) calculations were performed with the Gaussian 16 package.^[54] Geometry optimizations were performed via the spin-restricted Kohn-Sham (RKS) formalism with the BP86 functional of Becke and Perdew,^[55,56] including the D3 version of Grimme's dispersion (empiricaldispersion = GD3).^[57] The split valence basis set (Def2-SVP keyword in Gaussian) was used for the main group atoms,^[58,59] while for Si, Br, and Pd atoms, the quasi-relativistic Stuttgart/Dresden effective core potential with an associated valence contracted basis set (standard SDD keywords in Gaussian 16) was employed.^[60–62] Frequency calculations were performed to confirm the nature of the stationary points. Single point energy calculations were performed employing the B3LYP, hybrid GGA functional of Becke-Lee, Parr, and Yang,^[63–65] together with the D3 version of Grimme's dispersion, and the cc-pVTZ basis set,^[66] without and with solvent effects based on the polarizable solvation model density (SMD), variation of IEFPCM of Truhlar and co-workers,^[67] using toluene as the solvent (and hexane, acetonitrile, ethanol, DMF, and DMSO for comparison), omitting corrections of entropy and standard state of 1 M concentration in solution.^[68] For the Hal simulation, we employed the Hal model based on three Al and two Si units.^[69]

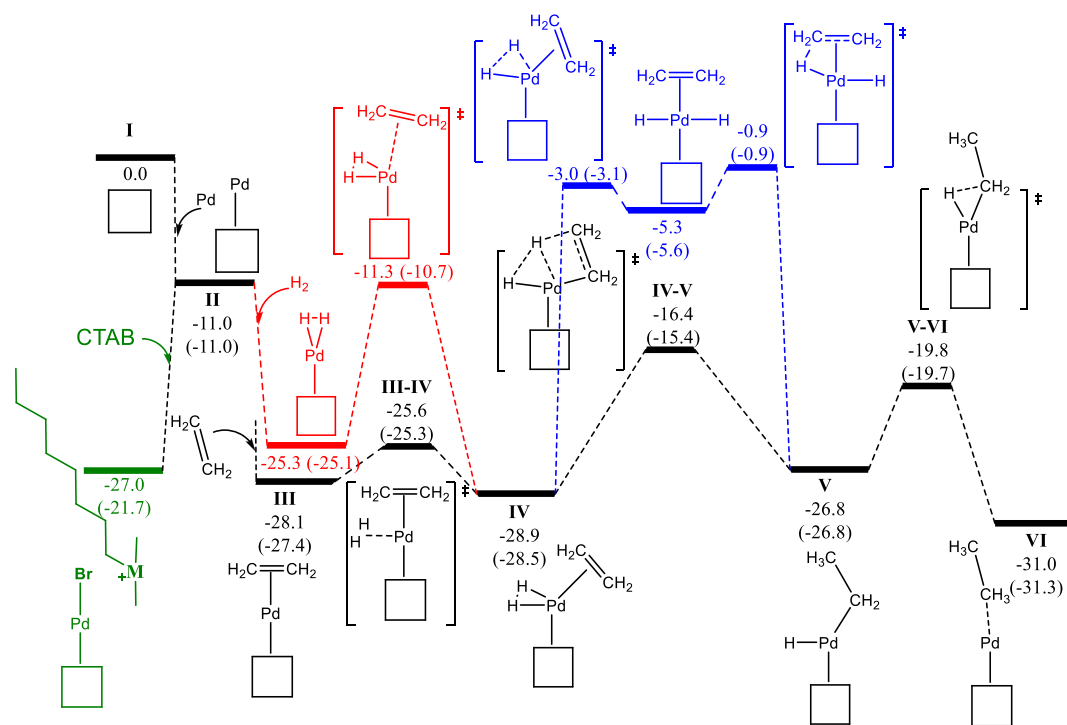
3 | RESULTS AND DISCUSSION

3.1 | Design of the catalysts

In our previous studies, we demonstrated that Hal is an efficient supporting material for the development of hydrogenation catalysts.^[44–46] Encouraged by the excellent performance of Hal, we decided to elucidate the effect of hydrophobicity of Hal on its catalytic activity. To tune the hydrophobicity of the outer surface of Hal that is negatively charged, a cationic surfactant, CTAB, was applied, and three samples were prepared. In the standard sample, Hal/Pd, Pd nanoparticles were immobilized on unmodified Hal.^[70] In the second sample, Hal/CTAB/Pd, Hal outer surface was first modified with CTAB, and then the resultant hydrophobic Hal was used as a support for the stabilization of Pd nanoparticles. Finally, to elucidate whether the order of introduction of CTAB can affect the activity of the resultant catalyst, a third sample, Hal/Pd/CTAB, was also prepared, in which Hal was first palladated and then treated with CTAB.

3.2 | Computational study

To distinguish which is the role of CTAB on the hydrogenation of olefins, DFT calculations were performed to



SCHEME 2 Relative energy profile (in kcal/mol) in gas phase at the B3LYP-D3BJ/cc-pVTZ~sdd//BP86-D3BJ/Def2SVP ~ sdd level of theory (in parenthesis including explicit solvent effects by solvation model density [SMD] [hexane]) of the ethylene hydrogenation via Pd-Hal catalyst (in red and blue alternative pathways; in green the interaction of cetrimonium bromide [CTAB])

unveil the reaction mechanism with ethylene as alkene substrate (see Scheme 2) and find out where CTAB participates. The first stage is search of the best coordination of the Pd(0) particle on Hal. The next step is alternative and allows the coordination of an ethylene or hydrogen molecule. Both types of substrate coordination are thermodynamically favored, but even more with the alkene, by 2.8 kcal/mol. Either way, then overcoming a transition state both reaction pathways converge at the same intermediate where hydrogen and olefin are bound to the palladium. It should be mentioned; however, that just as hydrogen coordination means a destabilization of only 2.5 kcal/mol. The olefin coordination is significantly hampered with an energy barrier of 14.0 kcal/mol. From the intermediate where they converge, two H-transfers lead to the formation of ethane, overcoming energy barriers of 12.5 and 7.0 kcal/mol, respectively. Thus, the first of the two is the rate determining step (rds). It should be noted, however, that heterolytic rupture of H₂ on the palladium before the two H-transfers has also been studied, but this pathway is kinetically demanding, with a cost of at least 28.0 kcal/mol. It is a minimum because the first of the two transition states could not be located, corresponding to the breaking of the H–H bond, and could only be approximated from a reaction coordinate. However, this is not important because the second

transition state of this alternative path is 15.5 kcal/mol above in energy. On the other hand, the addition of CTAB was studied over the course of the reaction pathway, and it is only explicitly significant when the palladium is less coordinated. The problem is clear as this favorable interaction would slow hydrogenation, in fact being more favorable by 1.7 kcal/mol than the insertion of hydrogen on the palladium, but still 1.1 kcal/mol less favored than the interaction with alkene. The values denote that CTAB will be a drawback for the reaction as the interaction with the palladium makes hydrogenation catalysis difficult, and not only at the beginning, but throughout the reaction profile.

Given the competition between the coordination of the two substrates, as well as the CTAB on the palladium, this interaction has also been studied in Scheme 2 including the solvent effects produced by hexane. Whereas there are no significant differences in the reaction pathway, relatively the interaction of the CTAB becomes significantly less favored. In fact, the value is 21.7 kcal/mol with respect to Hal as a reference species and thus 3.4 and 6.7 kcal/mol less stable than the molecular hydrogen or ethylene insertions. The coexistence of CTAB on the first sphere around the metal is not possible once any of the substrates bonds to the metal.

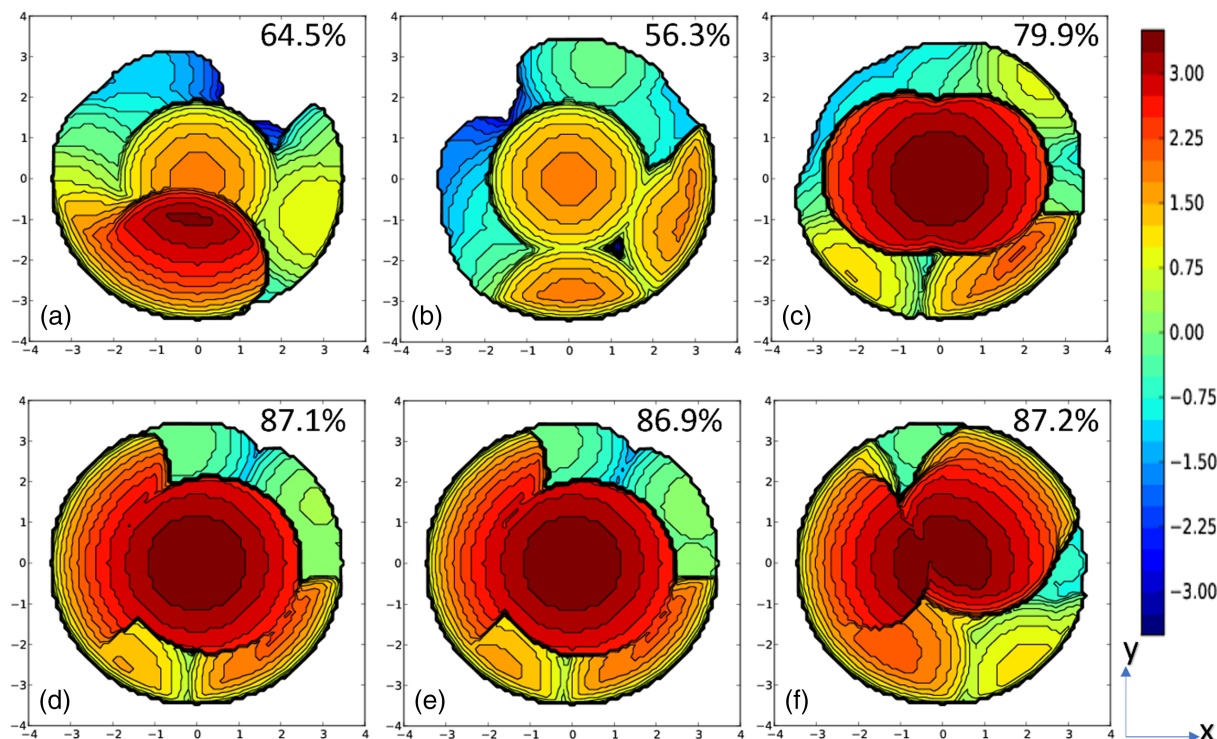


FIGURE 1 %V_{Bur} and steric maps on the metal center bonded to the halloysite: (a) empty, (b) with H₂, (c) with C₂H₄, and (d) with cetrimonium bromide (CTAB), (e) CTAB + H₂, (f) CTAB + C₂H₄ (xy plane, with the palladium placed in the center and the z-axis the oxygen bonded to palladium, including the oxygen of the closest methoxy group in the xz plane. Curves are given in Å, with a radius of 3.5 Å)

To be able to find out to what extent the CTAB is occupied by the palladium nanoparticle, the steric maps of Cavallo and coworkers are included in Figure 1.^[71,72] Also, the orientation of *x*-, *y*-, and *z*-axes for the steric maps is further detailed in Figure S1. In addition to the qualitative detail of the steric maps, the %V_{Bur} around the metal then allows to quantify the employability by substrates that can interact with it.^[73] First, it should be noted that the entry of H₂ if the palladium is simply attached to the metal is a significant change in the metal center and even decreases as coordination causes the palladium to leave the cavity, which is provided by halloysite, in order to coordinate with H₂, and consequently the %V_{Bur} decreases from 64.5% to 56.3%.^[74] Then, the %V_{Bur} without the CTAB around the metal implies a change from 64.5% to 79.9% once the olefin binds to it. If, on the other hand, we have the CTAB, there is an invariability because the %V_{Bur} is 87.1 and 87.2%, respectively,^[75] and the asymmetry even could not help at any less occupied quadrant.^[76] Therefore, there is a total invariability, as the metal center is virtually sequestered,^[77] especially by a bromine that also provides additional electron density with respect to olefin or molecular hydrogen. In fact, the coexistence of H₂ with the CTAB would be possible, although to the detriment of the substrate, because it is not coordinated in the metal center, but as an adduct, with a Pd^{II}H distance not less than 2.9 Å; therefore, in the background denying, a covalent interaction with the metal (the Mayer Bond Order^[78,79] is only 0.107 compared with 0.782 with the Pd^{II}Br).^[66]

Concluding the results of molecular simulation section, the presence of CTAB is detrimental to hydrogenation yield, from both energy and steric points of view. To shed light on the capability of CTAB containing catalyst, it was prepared and surveyed in PAO hydrofinishing. Also, the efficiency of this catalyst was compared with blank catalyst composed of bare Hal/Pd system.

3.3 | Hydrofinishing of the PAO using the as-prepared catalysts: Investigation of the reaction parameters using one-factor-at-a-time (OFAT) method

The catalytic activity of the three catalysts has been studied and compared for the hydrofinishing of PAO. Before comparing the activity of the developed catalysts, the effects of the reaction parameters (temperature, catalyst loading, and hydrogen pressure) have been studied by using the standard sample, Hal/Pd, as a catalyst. To this purpose, “one-factor-at-a-time” (OFAT) method has been applied. More precisely, the effect of each parameter was

investigated by varying that parameter, while keeping others constant.

3.3.1 | Effect of reaction temperature

To evaluate the effect of the reaction temperature, PAO hydrofinishing was performed in the presence of 5 wt.% catalyst at a hydrogen pressure of (8 bar) at different temperatures (100°C–140°C). The results (Figure S2) approved that hydrofinishing was not efficient at low temperatures and increase of temperature from 100°C to 130°C significantly affected the reaction yield. It is worth noting that increase of the reaction temperature from 130°C to 140°C was not effective. Hence, the optimum value for the hydrofinishing temperature was found to be 130°C.

3.3.2 | Effect of hydrogen pressure

To evaluate the effect of hydrogen pressure on the yield of hydrofinishing, the yields of PAO hydrofinishing at different hydrogen pressures (5–9 bar) were measured and compared (Figure S3). It was found that hydrogen pressure was a key factor and influenced the reaction yield remarkably. In fact, hydrofinishing reaction did not proceed efficiently at low hydrogen pressures and led to low to moderate yields. However, increase of this parameter to 8 bar resulted in increase of the yield of the reaction to 98%. Further increase of hydrogen pressure, however, was not influential, and 8 bar was selected as the optimum value for hydrogen pressure.

3.3.3 | Effect of catalyst loading

Finally, the investigation of the effect of catalyst loading was carried out to obtain the optimum amount of this parameter. To this purpose, hydrofinishing of PAO was performed in the presence of 2–6 wt.% Hal/Pd. The comparison of the yields of the reactions (Figure S4) indicated that upon increase of the catalyst content from 2 to 5 wt.%, the yield of the reaction increased, while further increase to 6 wt.% was ineffective. Based on these results, the optimum condition for hydrofinishing reaction was using 5 wt.% catalyst, hydrogen pressure of 8 bar at 130°C. ¹HNMR spectra of unhydrogenated PAO and the one hydrogenated under optimum reaction conditions are depicted in Figure 2. As can be seen in the spectrum of the hydrogenated sample, the peaks at 1.96 and 4.5–5.5 ppm (corresponding to the allyl and vinyl H moieties, respectively) disappeared.

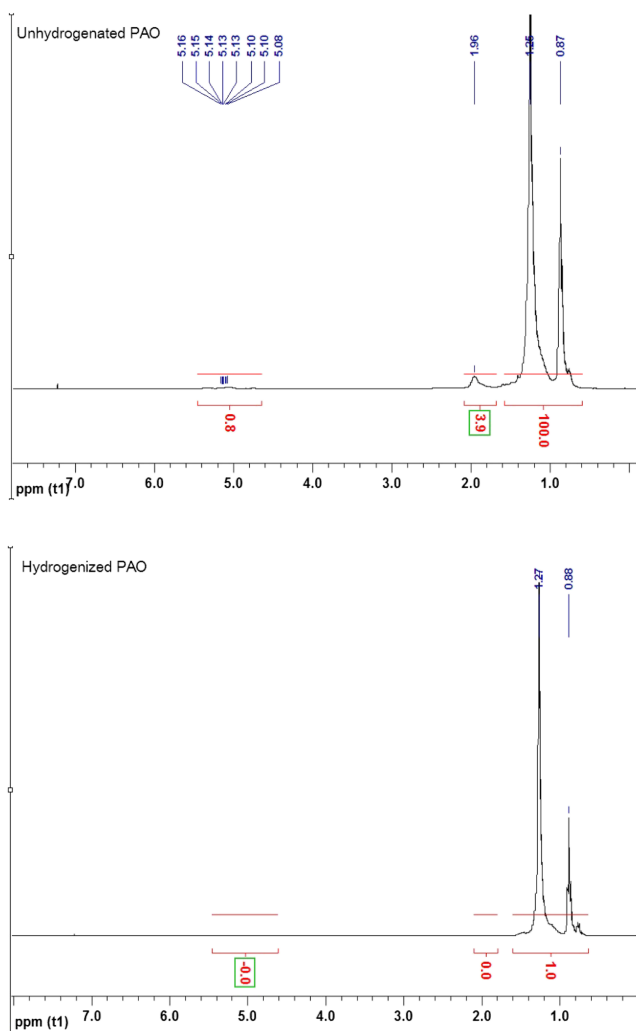


FIGURE 2 Nuclear magnetic resonance (^1H NMR) spectra of unhydrogenated (above) and hydrogenated (below) polyalphaolefin (PAO) at catalyst loading of 5 wt.%, hydrogen pressure of 8 bar and temperature of 130°C

3.4 | Comparison of the catalytic activities of the catalysts

Having the optimum reaction parameters in hand, the catalytic activity of the three synthesized catalysts has been compared for PAO hydrofinishing under the optimized conditions. Interestingly, the results implied that the order of the activity of the as-prepared catalysts was as follows: Hal/Pd > Hal/Pd/CTAB > Hal/CTAB/Pd. Experimentally obtained decrement of the catalytic performance by CTAB presence confirmed well the energy path of the hydrogenation reaction obtained from molecular simulations, in which CTAB via interaction with active Pd species, decreased their efficiency.

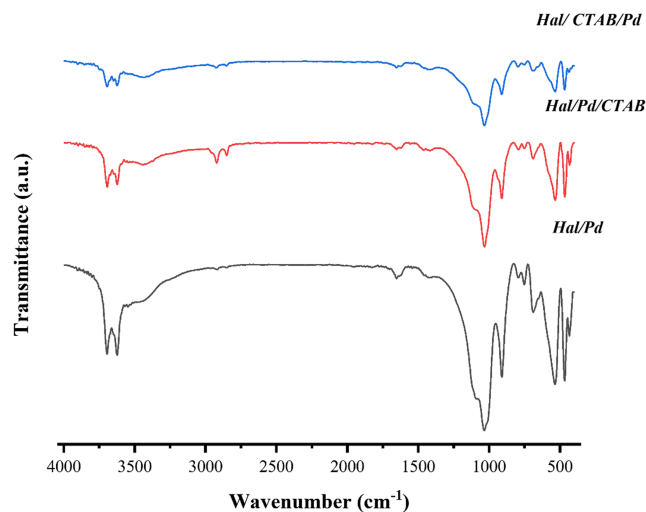


FIGURE 3 Fourier transform infrared (FTIR) spectra of the as-prepared catalysts

3.4.1 | Origin of the differences of the activity of the catalysts

To investigate the origin of the differences of the catalytic activity of the as-prepared catalysts, they have been characterized, and their properties have been compared.

To confirm conjugation of CTAB in Hal/CTAB/Pd and Hal/Pd/CTAB samples, all three samples were analyzed via FTIR spectroscopy. In Figure 3, FTIR spectra of Hal/Pd sample showed the characteristic absorbance bands of Hal at 3694 and 3627 cm^{-1} that is due to the internal $-\text{OH}$ groups, 1031 cm^{-1} that is assigned of $\text{Si}-\text{O}$ stretching and 540 cm^{-1} that is indicative of $\text{Al}-\text{O}-\text{Si}$ vibration.^[80] In the FTIR spectra of Hal/CTAB/Pd and Hal/Pd/CTAB samples, all of the aforementioned characteristic bands can be detected, confirming the stability of Hal structure. However, in these two samples, an additional band at 2942 cm^{-1} can be observed that is assigned to the $-\text{CH}_2$ stretching of the alkyl chain of CTAB. Quantitative studies also approved that the quantity of CTAB in Hal/Pd/CTAB is higher than Hal/CTAB/Pd.

To further approve the incorporation of CTAB and estimate the content of CTAB in Hal/CTAB/Pd and Hal/Pd/CTAB, TGA was applied. As depicted in Figure 4, in both TG curves, three weight losses can be detected. Two of the observed weight losses are attributed to loss of water and Hal dehydroxylation ($\sim 130^\circ\text{C}$ and 540°C , respectively).^[81,82] In the Hal/CTAB/Pd sample, the third weight loss appeared at 250°C ($\sim 2\text{ wt.}\%$), while in Hal/Pd/CTAB sample, this weight loss is detected at $240\text{--}320^\circ\text{C}$ ($\sim 10\text{ wt.}\%$). These results are in good accordance with the FTIR results and stated that synthetic procedure can affect the content of CTAB in the catalyst. In fact, in

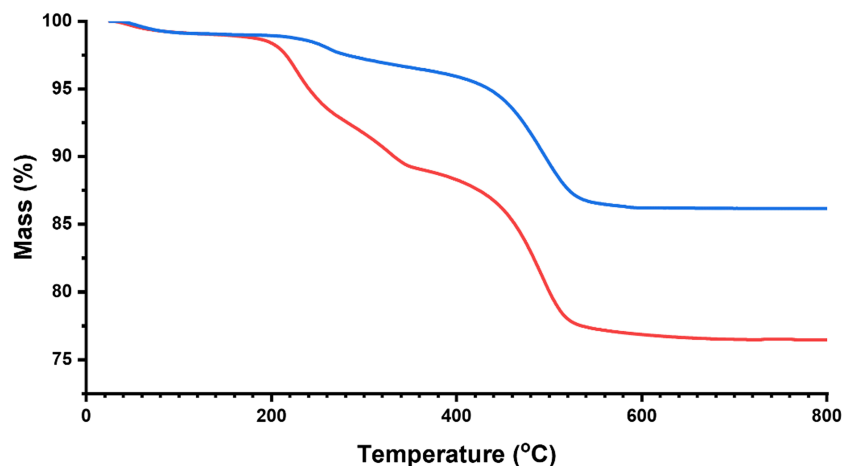


FIGURE 4 Thermogravimetric (TG) curves of the as-prepared halloysite (Hal)/Pd/cetrimonium bromide (CTAB) (red) and Hal/CTAB/Pd (blue)

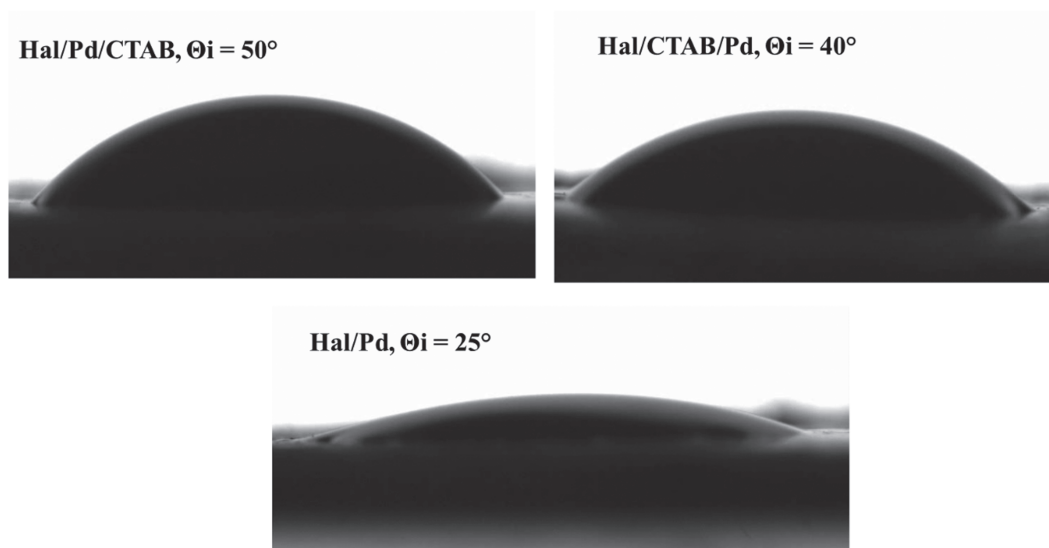


FIGURE 5 Water contact angle of the as-prepared catalysts

Hal/CTAB/Pd sample, in which palladation is conducted after incorporation of CTAB, loading of CTAB is significantly lower than that of Hal/Pd/CTAB. This can be due to the several washing steps used for the immobilization of Pd nanoparticles.

As the content of CTAB in Hal/CTAB/Pd and Hal/Pd/CTAB is different, it is expected that the hydrophobicity of these two samples differs. To elucidate this issue, the hydrophobicity of the as-prepared samples has been evaluated by contact angle measurements (Θ_i). As depicted in Figure 5, by treating Hal with CTAB, the hydrophobicity of the samples and consequently Θ_i values increased. It was also found that the hydrophobicity of Hal/Pd/CTAB was higher than that of Hal/CTAB/Pd.

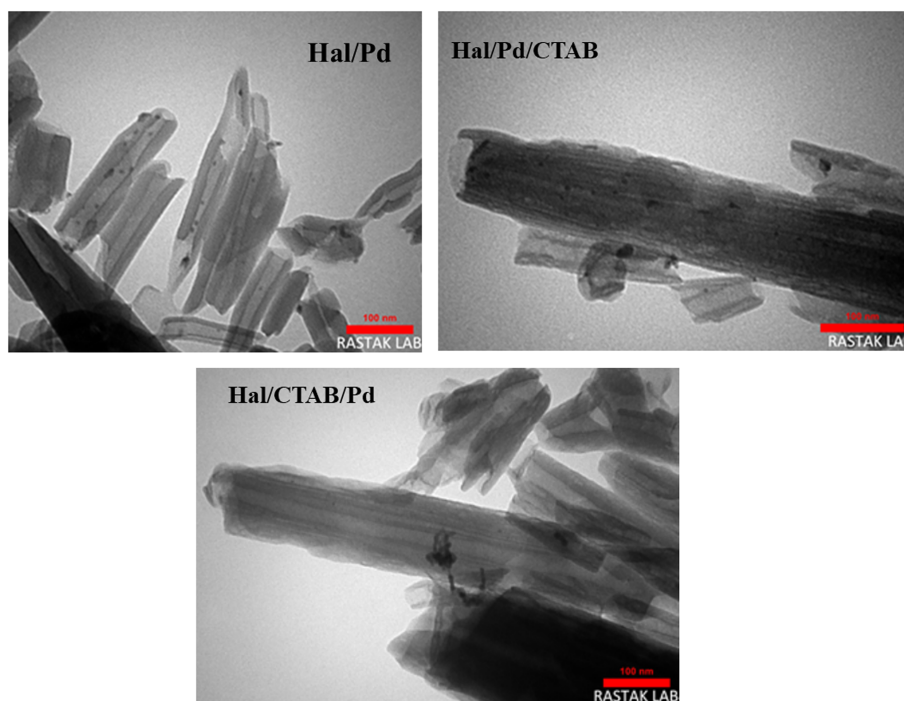
As one of the most important features of the catalysts that can affect the catalytic activity is Pd loading, all three samples have been subjected to ICP analysis. The results

indicated that the Pd loading in the catalysts follows the order of Hal/Pd/CTAB (1.2 wt.%) \approx Hal/Pd (\sim 1.2 wt.%) $>$ Hal/CTAB/Pd (0.8 wt.%). These results clearly established that the treatment of Hal with CTAB prior to palladation is detrimental to the Pd loading and led to the catalyst with a low Pd content. This issue is due to the electrostatic repulsion between the Pd salt and the hydrophobic Hal.

As another determinant on the catalytic activity is the dispersion of the catalytic active species, all three samples have been characterized via TEM. As shown in Figure 6, Pd nanoparticles have been aggregated in Hal/CTAB/Pd. This issue as long with low Pd content of this sample can justify its low catalytic activity. Regarding the two other samples, Pd nanoparticles were found to have homogeneously dispersed on Hal.

Next, the zeta potential value of the three as-prepared catalysts was estimated. This value increased in the

FIGURE 6 Transmission electronic microscopy (TEM) images of the as-prepared catalysts



following order: Hal/Pd/CTAB (18.3 mV) > Hal/CTAB/Pd (−20 mV) > Hal/Pd (−33 mV). As the electric charge of the exterior surface of Hal is negative, it is quite expectable that the CTAB-free sample, Hal/Pd, has the lowest zeta potential value. In Hal/Pd/CTAB and Hal/CTAB/Pd, which contain surfactant, CTAB neutralized the negative charge of Hal and then led to the increase of zeta potential value compared with Hal/Pd. As proven by TGA and FTIR, the content of CTAB in Hal/Pd/CTAB was higher; hence, the zeta potential value of Hal/Pd/CTAB is higher than that of Hal/CTAB/Pd.

3.5 | Further characterization of Hal/Pd

Finding Hal/Pd as the catalyst of choice, it was further characterized via XRD, BET, and elemental mapping analysis.

Elemental mapping analysis of Hal/Pd in Figure 7 implies that apart from Si, Al, and O atoms that are representative of Hal, Pd atom is also present in the structure of the catalyst. It was observed that the dispersion of Pd NPs was uniform.

XRD analysis of Hal/Pd was also conducted to elucidate the crystal phase of Hal/Pd in Figure 8. According to the literature,^[83] the observed peaks at $2\theta = 19.9^\circ, 24.4^\circ, 26.6^\circ, 38.5^\circ, 55.2^\circ, 62.5^\circ, 73.9^\circ,$ and 77.4° are assigned to the characteristic bands of Hal (JCPDS No. 29–1487). Noteworthy, the absence of the characteristic peaks of Pd

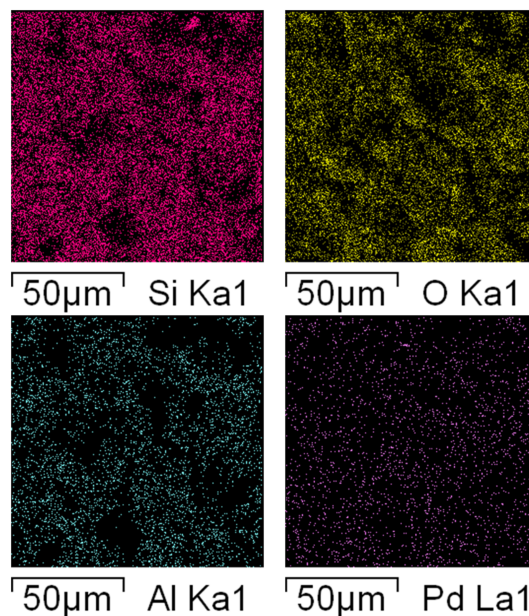


FIGURE 7 Elemental mapping analysis of halloysite (Hal)/Pd

nanoparticles can be attributed to the low loading and high dispersion of these particles.^[84]

The comparison of the specific surface area of the pristine Hal and Hal/Pd showed that this value decreased slightly from 49.2 to 44.3 m²/g upon immobilization of Pd nanoparticles. On the other hand, the value of total pore volume for both samples, Hal and Hal/Pd, was almost similar (0.19 cm³/g). These results indicate that Pd nanoparticles were formed on the exterior surface of

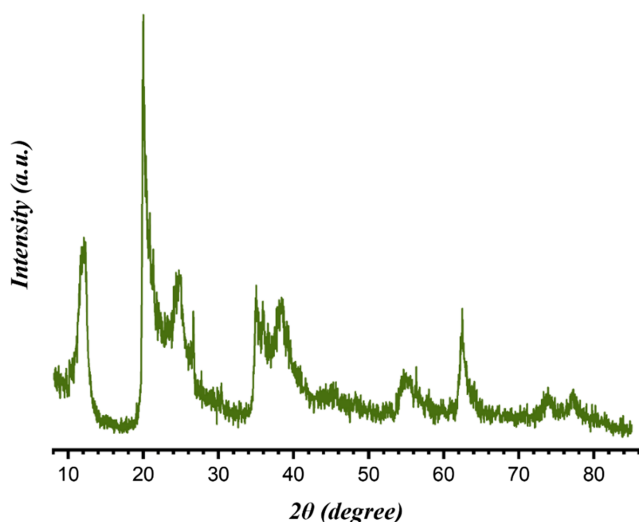


FIGURE 8 X-ray diffraction (XRD) pattern of Hal/Pd

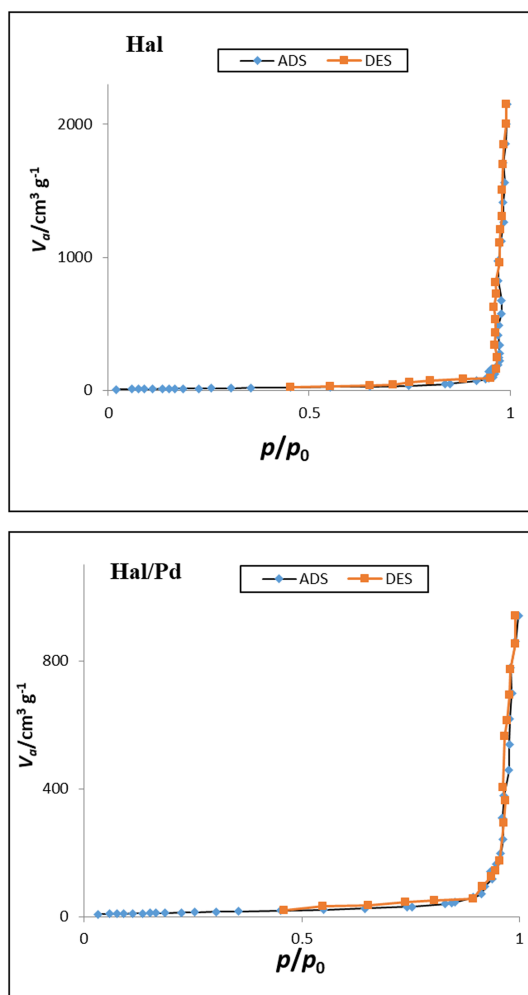


FIGURE 9 Nitrogen adsorption-desorption isotherms of halloysite (Hal) and Hal/Pd

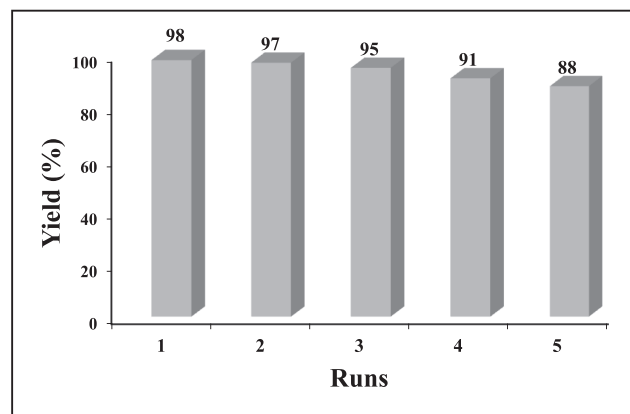


FIGURE 10 Recycling of halloysite (Hal)/Pd for hydrofinishing of polyalphaolefin (PAO). Reaction condition: $T = 130^{\circ}\text{C}$, catalyst dosage = 5 wt.% and $P_{\text{H}_2} = 8$ bar

Hal. As shown in Figure 9, the N_2 adsorption-desorption isotherms of both Hal and Hal/Pd, are of type IV with H3 hysteresis loop, implying the mesoporous structure with slit-like pores.^[85]

3.6 | Recyclability

The recyclability of Hal/Pd was also investigated by reusing the recovered catalyst for several reaction runs. In more detail, at the end of the first run of hydrofinishing, Hal/Pd was separated via centrifugation, recovered, and then reused for the next run of hydrofinishing. In Figure 10, the yields of hydrofinishing for five consecutive runs are depicted. As illustrated, the reused Hal/Pd almost maintained its catalytic activity, and only slight loss of the catalytic activity was observed after each run. Characterization of the reused Hal/Pd after the fifth run via ICP approved insignificant leaching of Pd nanoparticles from Hal (~ 1 wt.% of initial Pd content). It is worth noting that hot filtration test was also conducted to investigate the heterogeneous nature of the catalysis, and the results indicated that the catalysis was heterogeneous and Pd nanoparticles were remained stabilized on the support in the course of hydrogenation reaction.

4 | CONCLUSIONS

In summary, to study the effect of hydrophobicity of Hal on its performance as a support for Pd nanoparticles, three catalysts with different hydrophobicity, that is, Hal/Pd, Hal/Pd/CTAB, and Hal/CTAB/Pd, were prepared, and their catalytic activity for hydrofinishing of PAO was examined. Both experimental and

computational results indicated that introduction of CTAB had a detrimental effect on the catalytic activity of the catalyst and Hal/Pd showed the best catalytic activity. In fact, characterization of the three samples confirms that not only the presence of CTAB could affect the catalytic activity but also the synthetic procedure and the order of incorporation of Pd nanoparticles and CTAB were influential on the catalytic performance of the catalyst. According to the results, in Hal/CTAB/Pd, introduction of CTAB prior to Pd immobilization led to low Pd loading, particle aggregation, and consequently the lowest catalytic activity. However, no linear relationship with the catalytic activities was achieved.

ACKNOWLEDGMENTS

Samahe Sadjadi and Naeimeh Bahri-Laleh are thankful to Iran Polymer and Petrochemical Institute for financial support. Albert Poater is a Serra Hünter Fellow and ICREA Academia Prize 2019 and thanks the Spanish MINECO for project ref. PGC2018-097722-B-I00.






AUTHOR CONTRIBUTIONS

Arash Shams: Data curation; formal analysis; investigation. **Samahe Sadjadi:** Conceptualization; funding acquisition; methodology; resources; supervision. **Josep Duran:** Formal analysis; investigation. **Silvia Simon:** Formal analysis; investigation. **Albert Poater:** Conceptualization; funding acquisition; methodology; resources; supervision. **Naeimeh Bahri-Laleh:** Conceptualization; funding acquisition; methodology; resources; supervision.

CONFLICT OF INTEREST

There is no conflict to declare.

ORCID

Arash Shams  <https://orcid.org/0000-0002-6426-7703>
 Samahe Sadjadi  <https://orcid.org/0000-0002-6884-4328>
 Josep Duran  <https://orcid.org/0000-0003-2121-6364>
 Silvia Simon  <https://orcid.org/0000-0003-4935-1824>
 Albert Poater  <https://orcid.org/0000-0002-8997-2599>
 Naeimeh Bahri-Laleh  <https://orcid.org/0000-0002-0925-5363>

REFERENCES

- [1] G. J. Hutchings, *Faraday Discuss.* **2021**, 229, 9.
- [2] A. Corma, H. García, *Chem. Rev.* **2003**, 103, 4307.
- [3] N. Bahri-Laleh, A. Hanifpour, S. A. Mirmohammadi, A. Poater, M. Nekoomanesh-Haghighi, G. Talarico, L. Cavallo, *Prog. Polym. Sci.* **2018**, 84, 89.
- [4] S. K. Kaiser, Z. Chen, D. F. Akl, S. Mitchell, J. Pérez-Ramírez, *Chem. Rev.* **2020**, 120, 11703.
- [5] M. R. Axet, O. Dechy-Cabaret, J. Durand, M. Gouygou, P. Serp, *Coord. Chem. Rev.* **2016**, 308, 236.
- [6] G. Lazzara, G. Cavallaro, A. Panchal, R. Fakhruddin, A. Stavitskaya, V. Vinokurov, Y. Lvov, *Curr. Opin. Colloid Interface Sci.* **2018**, 35, 42.
- [7] G. Cavallaro, L. Chiappisi, P. Pasbakhsh, M. Gradzielski, G. Lazzara, *Appl. Clay Sci.* **2018**, 160, 71.
- [8] H. Wang, D. Wu, X. Li, P. Huo, *J. Mater. Sci.: Mater. Electron.* **2019**, 30, 19126.
- [9] V. A. Vinokurov, A. V. Stavitskaya, E. V. Ivanov, P. A. Gushchin, D. V. Kozlov, A. Y. Kurenkova, P. A. Kolinko, E. A. Kozlova, Y. M. Lvov, *ACS Sustainable Chem. Eng.* **2017**, 5, 11316.
- [10] L. Deng, P. Yuan, D. Liu, P. Du, J. Zhou, Y. Wei, Y. Song, Y. Liu, *Appl. Clay Sci.* **2019**, 181, 105240.
- [11] V. Vinokurov, A. Stavitskaya, A. Glotov, A. Ostudin, M. Sosna, P. Gushchin, Y. Darrat, Y. Lvov, *J. Solid State Chem.* **2018**, 268, 182.
- [12] R. J. Smith, K. M. Holder, S. Ruiz, W. Hahn, Y. Song, Y. M. Lvov, J. C. Grunlan, *Adv. Funct. Mater.* **2018**, 28, 1703289.
- [13] T. Yu, L. T. Swientoniewski, M. Omarova, M.-C. Li, I. I. Negulescu, N. Jiang, O. A. Darvish, A. Panchal, D. A. Blake, Q. Wu, Y. M. Lvov, V. T. John, D. Zhang, *ACS Appl. Mater. Interfaces* **2019**, 11, 27944.
- [14] G. Cavallaro, G. Lazzara, S. Milioto, F. Parisi, *Chem. Rec.* **2018**, 18, 1.
- [15] I. Anastopoulos, A. Mittal, M. Usman, J. Mittal, G. Yu, A. Núñez-Delgado, M. Kornaros, *J. Mol. Liq.* **2018**, 269, 855.
- [16] C. E. Tas, S. Hendessi, M. Baysal, S. Unal, F. C. Cebeci, Y. Z. Menciloglu, H. Unal, *Food Bioprocess. Tech.* **2017**, 10, 789.
- [17] L. Lisuzzo, G. Cavallaro, S. Milioto, G. Lazzara, *J. Colloid Interface Sci.* **2022**, 608, 424.
- [18] G. Lazzara, G. Cavallaro, A. Panchal, R. Fakhruddin, A. Stavitskaya, V. Vinokurov, Y. Lvov, *Curr. Opin. Colloid Interface Sci.* **2018**, 35, 42.
- [19] P. Yuan, D. Tan, F. Annabi-Bergaya, *Appl. Clay Sci.* **2015**, 112–113, 75.
- [20] L.-L. Deng, P. Yuan, D. Liu, F. Annabi-Bergaya, J. Zhou, F. Chen, Z. Liu, *Appl. Clay Sci.* **2017**, 143, 184.
- [21] Y. Wei, P. Yuan, D. Liu, D. Losic, D. Tan, F. Chen, H. Liu, J. Zhou, P. Du, Y. Song, *Chem. Commun.* **2019**, 55, 2110.
- [22] M. Massaro, G. Lazzara, S. Milioto, R. Noto, S. Riela, *J. Mater. Chem. B* **2017**, 5, 2867.
- [23] M. Massaro, C. G. Colletti, G. Buscemi, S. Cataldo, S. Guernelli, G. Lazzara, L. F. Liotta, F. Parisi, A. Pettignano, S. Riela, *New J. Chem.* **2018**, 42, 13938.
- [24] S. Dehghani, S. Sadjadi, N. Bahri-Laleh, M. Nekoomanesh-Haghighi, A. Poater, *Appl. Organomet. Chem.* **2019**, 33, e4891.
- [25] L. Lisuzzo, G. Cavallaro, S. Milioto, G. Lazzara, *Appl. Clay Sci.* **2020**, 185, 105416.
- [26] N. Danyliuk, J. Tomaszewska, T. Tatarchuk, *J. Mol. Liq.* **2020**, 309, 113077.
- [27] S. Sadjadi, N. Abedian-Dehaghani, F. Koohestani, M. M. Heravi, *Inorg. Chem. Commun.* **2021**, 133, 108955.
- [28] Z. Zhu, D. Ding, Y. Zhang, Y. Zhang, *Appl. Clay Sci.* **2020**, 196, 105761.
- [29] M. Massaro, C. G. Colletti, B. Fiore, V. la Parola, G. Lazzara, S. Guernelli, N. Zaccheroni, S. Riela, *Appl. Organomet. Chem.* **2019**, 33, e4665.

- [30] M. J. Baruah, T. J. Bora, R. Dutta, S. Roy, A. K. Guha, K. K. Bania, *Mol. Catal.* **2021**, *515*, 111858.
- [31] A. Mahajan, P. Gupta, *New J. Chem.* **2020**, *44*, 12897.
- [32] J. Jin, J. Ouyang, H. Yang, *Nanoscale Res. Lett.* **2017**, *12*, 240.
- [33] A. Hanifpour, N. Bahri-Laleh, A. Mohebbi, M. Nekoomanesh-Haghighi, *Iran Polym. J.* **2021**, *31*, 107.
- [34] A. Hanifpour, M. H. Gargari, M. R. R. Darouk, Z. Kalantari, N. Bahri-Laleh, *Polyolefins J.* **2021**, *8*, 31.
- [35] T. H. Ritter, H. G. Alt, *Polyolefins J.* **2020**, *7*, 79.
- [36] A. Hanifpour, N. Bahri-Laleh, M. Nekoomanesh-Haghighi, A. Poater, *Green Chem.* **2020**, *22*, 4617.
- [37] A. Hanifpour, N. Bahri-Laleh, M. Nekoomanesh-Haghighi, A. Poater, *Mol. Catal.* **2020**, *493*, 111047.
- [38] T. B. Mikenas, V. A. Zakharov, M. A. Matsko, *Iran Polym. J.* **2022**, *31*, 27. <https://doi.org/10.1007/s13726-021-01004-w>
- [39] E. O. C. Greiner, Y. Inoguchi, *Chemical Economics Handbook: Linear alpha-Olefins*, SRI Consulting, Menlo Park, CA **2010**.
- [40] A. Rahbar, N. Bahri-Laleh, M. Nekoomanesh-Haghighi, *Fuel* **2021**, *302*, 121111.
- [41] A. Jalali, M. Nekoomanesh-Haghighi, S. Dehghani, N. Bahri-Laleh, *Appl. Organomet. Chem.* **2020**, *34*, e5338.
- [42] X. Zhang, M. Fevre, G. O. Jones, R. M. Waymouth, *Chem. Rev.* **2018**, *118*, 839.
- [43] M. Fallah, N. Bahri-Laleh, K. Didehban, A. Poater, *Appl. Organomet. Chem.* **2020**, *34*, e5333.
- [44] S. Sadjadi, F. Koohestani, G. Pareras, M. Nekoomanesh-Haghighi, N. Bahri-Laleh, A. Poater, *J. Mol. Liq.* **2021**, *331*, 115740.
- [45] M. Tabrizi, S. Sadjadi, G. Pareras, M. Nekoomanesh-Haghighi, N. Bahri-Laleh, A. Poater, *J. Colloid Interface Sci.* **2021**, *581*, 939.
- [46] S. Karimi, N. Bahri-Laleh, G. Pareras, S. Sadjadi, M. Nekoomanesh-Haghighi, A. Poater, *J. Ind. Eng. Chem.* **2021**, *97*, 441.
- [47] M. Alleshagh, S. Sadjadi, H. Arabi, N. Bahri-Laleh, E. Monflier, *Mater. Chem. Phys.* **2022**, *278*, 125506.
- [48] M. Mehdizadeh, S. Sadjadi, A. Poater, A. Mansouri, N. Bahri-Laleh, *J. Mol. Liq.* **2022**, *352*, 118675.
- [49] S. Gharajedaghi, Z. Mohamadnia, E. Ahmadi, M. Marefat, G. Pareras, S. Simon, A. Poater, N. Bahri-Laleh, *Mol. Catal.* **2021**, *509*, 111636.
- [50] A. Hanifpour, N. Bahri-Laleh, M. Nekoomanesh-Haghighi, A. Poater, *Appl. Organomet. Chem.* **2021**, *34*, e6227.
- [51] S. Sadjadi, M. Atai, *Appl. Organomet. Chem.* **2019**, *33*, e4776.
- [52] S. Sadjadi, *Appl. Organomet. Chem.* **2018**, *32*, e4211.
- [53] G. Cavallaro, G. Lazzara, S. Milioto, F. Parisi, *Langmuir* **2015**, *31*, 7472.
- [54] M. J. Frisch, G. W. Trucks, H. B. Schlegel, G. E. Scuseria, M. A. Robb, J. R. Cheeseman, G. Scalmani, V. Barone, B. Mennucci, G. A. Petersson, H. Nakatsuji, M. Caricato, X. Li, H. P. Hratchian, A. F. Izmaylov, J. Bloino, G. Zheng, J. L. Sonnenberg, M. Hada, M. Ehara, K. Toyota, R. Fukuda, J. Hasegawa, M. Ishida, T. Nakajima, Y. Honda, O. Kitao, H. Nakai, T. Vreven, J. A. Montgomery, J. E. Peralta, F. Ogliaro, M. Bearpark, J. J. Heyd, E. Brothers, K. N. Kudin, V. N. Staroverov, R. Kobayashi, J. Normand, K. Raghavachari, A. Rendell, J. C. Burant, S. S. Iyengar, J. Tomasi, M. Cossi, N. Rega, J. M. Millam, M. Klene, J. E. Knox, J. B. Cross, V. Bakken, C. Adamo, J. Jaramillo, R. Gomperts, R. E. Stratmann, O. Yazyev, A. J. Austin, R. Cammi, C. Pomelli, J. W. Ochterski, R. L. Martin, K. Morokuma, V. G. Zakrzewski, G. A. Voth, P. Salvador, J. J. Dannenberg, S. Dapprich, A. D. Daniels, Ö. Farkas, J. B. Foresman, J. V. Ortiz, J. Cioslowski, D. J. Fox, *Gaussian 16*, Gaussian Inc., Wallingford CT **2016**.
- [55] A. D. Becke, *Phys. Rev. A* **1988**, *38*, 3098.
- [56] J. P. Perdew, *Phys. Rev. B* **1986**, *33*, 8822.
- [57] S. Grimme, J. Antony, S. Ehrlich, H. Krieg, *J. Chem. Phys.* **2010**, *132*, 154104.
- [58] F. Weigend, R. Ahlrichs, *Phys. Chem. Chem. Phys.* **2005**, *7*, 3297.
- [59] F. Weigend, *Phys. Chem. Chem. Phys.* **2006**, *8*, 1057.
- [60] U. Häussermann, M. Dolg, H. Stoll, H. Preuss, P. Schwerdtfeger, R. Pitzer, *Mol. Phys.* **1993**, *78*, 1211.
- [61] W. Küchle, M. Dolg, H. Stoll, H. Preuss, *J. Chem. Phys.* **1994**, *100*, 7535.
- [62] T. Leininger, A. Nicklass, H. Stoll, M. Dolg, P. Schwerdtfeger, *J. Chem. Phys.* **1996**, *105*, 1052.
- [63] A. D. Becke, *J. Chem. Phys.* **1993**, *98*, 5648.
- [64] C. Lee, W. Yang, R. G. Parr, *Phys. Rev. B* **1988**, *37*, 785.
- [65] P. J. Stephens, F. J. Devlin, C. F. Chabalowski, M. J. Frisch, *J. Phys. Chem.* **1994**, *98*, 11623.
- [66] T. H. Dunning Jr., *J. Chem. Phys.* **1989**, *90*, 1007.
- [67] A. V. Marenich, C. J. Cramer, D. G. Truhlar, *J. Phys. Chem. B* **2009**, *113*, 6378.
- [68] L. Falivene, V. Barone, G. Talarico, *Mol. Catal.* **2018**, *452*, 138.
- [69] S. Sadjadi, N. Bahri-Laleh, *J. Porous Mater.* **2018**, *25*, 1.
- [70] T. Ataee-Kachouei, M. Nasr-Esfahani, I. Mohammadpoor-Baltork, V. Mirkhani, M. Moghadam, S. Tangestaninejad, B. Notash, *Appl. Organomet. Chem.* **2020**, *34*, e5948.
- [71] L. Falivene, R. Credendino, A. Poater, A. Petta, L. Serra, R. Oliva, V. Scarano, L. Cavallo, *Organometallics* **2016**, *35*, 2286.
- [72] L. Falivene, Z. Cao, A. Petta, L. Serra, A. Poater, R. Oliva, V. Scarano, L. Cavallo, *Nat. Chem.* **2019**, *11*, 872.
- [73] A. Poater, B. Cosenza, A. Correa, S. Giudice, F. Ragone, V. Scarano, L. Cavallo, *Eur. J. Inorg. Chem.* **2009**, *2009*, 1759.
- [74] J. Poater, M. Gimferrer, A. Poater, *Inorg. Chem.* **2018**, *57*, 6981.
- [75] M. Tomasini, J. Duran, S. Simon, L. M. Azofra, A. Poater, *Mol. Catal.* **2021**, *510*, 111692.
- [76] N. Bahri-Laleh, A. Poater, L. Cavallo, S. A. Mirmohammadi, *Dalton Trans.* **2014**, *43*, 15143.
- [77] N. Bahri-Laleh, S. Sadjadi, A. Poater, *J. Colloid Interface Sci.* **2018**, *531*, 421.
- [78] I. Mayer, *Chem. Phys. Lett.* **1983**, *97*, 270.
- [79] A. Poater, A. G. Saliner, M. Solà, L. Cavallo, A. P. Worth, *Expert Opin. Drug Deliv.* **2010**, *7*, 295.
- [80] J. Jin, L. Fu, H. Yang, J. Ouyang, *Sci. Rep.* **2015**, *5*, 12429.
- [81] S. Bordepong, D. Bhongsuwan, T. Pungrassami, T. Bhongsuwan, *Songklanakarin J. Sci. Technol.* **2011**, *33*, 599.
- [82] L. Zatta, J. E. F. da Costa Gardolinski, F. Wypych, *Appl. Clay Sci.* **2011**, *51*, 165.
- [83] S. Sadjadi, *Appl. Clay Sci.* **2020**, *189*, 105537.
- [84] S. Mallik, S. S. Dash, K. M. Parida, B. K. Mohapatra, *J. Colloid Interface Sci.* **2006**, *300*, 237.

[85] Y. H. Ahmad, A. T. Mohamed, S. Y. Al-Qaradawi, *Appl. Clay Sci.* **2021**, *201*, 105956.

SUPPORTING INFORMATION

Additional supporting information may be found in the online version of the article at the publisher's website.

How to cite this article: A. Shams, S. Sadjadi, J. Duran, S. Simon, A. Poater, N. Bahri-Laleh, *Appl Organomet Chem* **2022**, *36*(7), e6719. <https://doi.org/10.1002/aoc.6719>